Theoretical Prediction of Induction Period from Transient Pore Evolvement in Polyester-Based Microparticles

AIYING ZHAO,[1] S.K. HUNTER,[2] V.G.J. RODGERS[3]

[1]Department of Chemical and Biochemical Engineering, The University of Iowa, Iowa City, Iowa 52242

[2]Department of Obstetrics and Gynecology, Carver College of Medicine, The University of Iowa, Iowa City, Iowa 52241

[3]B2K Group (Biotransport & Bioreaction Kinetics Group), Department of Bioengineering, University of California, A237 Bourns Hall, Riverside, California

Received 6 May 2009; revised 25 February 2010; accepted 2 March 2010

Published online 13 May 2010 in Wiley InterScience (www.interscience.wiley.com). DOI 10.1002/jps.22167

ABSTRACT: A model was developed and compared to experimental results for prediction of the induction period during drug delivery from various compositions of biodegradable copolymer PLGA microparticles. The uniqueness of this model is that it considers transient pore evolvement and uses the kinetic parameters of polymer degradation, which are independent of experimental measurements of microparticle erosion, in its analysis. Delivery data from PLGA microparticles (50:50, 75:25, and 85:15) releasing ovalbumin (OVA, 46 kDa) and bovine serum albumin (BSA, 66 kDa) were determined and used as the model systems. Experimental measurements were carried out from 85 to 150 days depending on the PLGA characteristics. The predicted induction periods were approximately 45, 70, and 105 days for the release of both OVA and BSA from 50:50, 75:25, and 85:15 PLGA microparticles, respectively. Overall, these values were in very good agreement with experimentally estimated results. © 2010 Wiley-Liss, Inc. and the American Pharmacists Association J Pharm Sci 99:4477–4487, 2010

Keywords: mathematical modeling; induction time; polymer degradation; transient pore evolvement; bulk erosion kinetics; hindered transport; polyesters; microparticles; probabilistic model

INTRODUCTION

Polyester-based microparticles undergoing bulk erosion, especially poly lactic-*co*-glycolic acid (PLGA)-based microparticles are potential delivery vehicles for pulsatile release.[1–3] A number of factors influence the overall release profiles including water intrusion into the device, polymer degradation, diffusion of protein molecules and polymer degradation products, microenvironmental pH changes, osmotic effects, adsorption/desorption process,[4,5] and protein decomposition/denaturation.[6,7] Understanding the governing mechanisms can provide the foundation for predictability of long-term release profiles during controlled drug delivery. This can have particular significance for scenarios requiring rapid protocol adjustments for administration of a variety of vaccines.

As systems such as PLGA microparticles undergo bulk erosion, hydration is imminent and polymer chains are simultaneously cleaved throughout the microparticles. Thus, polymer degradation and transport processes are two major interacting factors in determining drug release profiles.[1,8,9] The inner morphologies of the microparticles under bulk erosion, which is related to polymer degradation and significantly influence various transport processes, have been found to be very complex and usually heterogeneous.[10–12] In addition, the spontaneous pore opening, closing and coalescence during erosion make it difficult to predict the transient pore structure of the microparticles.[13] The morphological limiting effect of polymer erosion is the main cause to the induction period (or dead time), which is defined as the time interval between two pulses in drug delivery. The induction period is one of the most important parameters in controlled drug release which largely determines the overall release profile. In addition to polymer erosion, other factors affect the induction period including geometric properties of the polymeric systems, such as particle size, size distribution and internal structure properties; physicochemical properties and molecular weight of the entrapped drug/protein. Geometric factors directly influence the availability of particle contact points, porosity, viscosity, and tortuosity of matrices, which of all determines the effective surface area. Effective

Correspondence to: V.G.J. Rodgers (Telephone: 951-827-6241; Fax: 951-827-6416; E-mail: victor.rodgers@ucr.edu)

Journal of Pharmaceutical Sciences, Vol. 99, 4477–4487 (2010)

surface area of the particles, including external surface area and internal surface area, plays an important role in the variation of induction period for a fixed formulation composition. Physicochemical properties and molecular weight of the entrapped drug/protein also affects polymer dissolution and pore evolvement, consequently influence the induction period. Large entrapped molecules tend to be associated with long induction period.

Recognizing this, characterization of the microparticle morphology was approached early on in drug delivery and a series of methods have been developed.[14–17] The hydrolysis kinetics of polyesters under various conditions has also been investigated. The molecular loss rate of copolymers was found to adhere well to pseudo-first-order kinetics.[3,18] This hydrolytic rate constants of polymers was found to be approximated using experimental results from gel permeation chromatography.[19]

The resulting transport of entrained solutes, such as proteins, in the microparticles under bulk erosion has also been studied through various approaches including hindered transport.[20–22] In particular, for drug delivery from polyester-based microparticles, the progress of hydrolysis and bulk mass loss have been correlated to the growth of existing pores and the generation of new pores.[10] Batycky first directly related pore growth to pore coalescence rate (k_{coal}),

$$R_{ave}(t) \propto k_{coal} t \tag{1}$$

where k_{coal} depends on polymer erosion and its value can be estimated through experimental observations.[23] Lemaire et al. followed this model and describes the transient pore size as a function of time by the approximation:

$$R_p(t) = kt + R_0 \tag{2}$$

in which k is a constant representing the erosion velocity and R_0 is the initial pore radius.[24] In addition, computational algorithms have also been developed to couple drug release with polymer degradation based on Monte Carlo techniques.[1,3,25] However, in previous models, the erosion coefficient, either k_{coal} or k, were determined directly from experimentally observed polymer erosion behavior.[23,24]

Nevertheless, theoretical prediction of drug delivery, particularly for the induction period for polyesters undergoing bulk erosion has not been, to our knowledge, directly related to the erosion kinetics and transient pore evolvement information that are independent of direct measurements from the degrading microparticle. Therefore, in this study, a mathematical model is developed to directly predict the induction period from molecular properties of original polymer and erosion kinetics data that are independent of the microparticle empirical degradation data.

Here predictability of induction period is emphasized for potential vaccine applications. The pore evolvement over time and the transport properties of protein molecules in pores with increasing pore diameter is addressed using hindered transport theory.[21,22] The model results are compared to experimental release result of ovalbumin (OVA, 46 kDa) and bovine serum albumin (BSA, 66 kDa) from PLGA of ratios, 50:50, 75:25, and 85:15.

GENERAL MODEL DEVELOPMENT

Pore Generation and Growth in the Degrading Microparticles

As a first approximation, the model begins by assuming that the solute release process from PLGA microparticles can be modeled as a constant–activity cylindrical reservoir system. This approximation is reasonable when addressing primarily the induction period where overall pore distribution in the microparticle is relatively constant and, by nature of the spherical particle shape, the mass of the encapsulated material resides primarily near the outer particle radius. In addition, since water intrusion is relatively fast for PLGA particles that undergo bulk erosion, a major factor that influences polymer degradation kinetics is the solubility of the entrapped drug. In the case of water-soluble proteins, many factors determine its solubility.[26,27] In addition, the released protein molecules and polymer degradation products will affect the pore microenvironment, such as pH and viscosity of the medium, which will affect the polymer degradation kinetics. The autocatalysis phenomenon has been acknowledged by many researchers for polyester-based microparticles as well; that is, the degradation products of PLGA decrease the pH of microenvironment and catalyze the degradation of polymer. In the general model development, the effect of drug/protein to the induction period will be described by hindered transport through water-filled pores; the effect of PLGA autocatalysis can be coupled in the first-order coefficient of polymer degradation kinetics. Thus the PLGA microparticles can be modeled as a constant–activity cylindrical reservoir system. We consider only pore evolvement, and reduce our model to a straight pore in a spherical particle with pore size growing at the degradation time t (Fig. 1). For an arbitrary erodible polymer, the degradation products include monomers and oligomers. Therefore, to quantify the transient pore size, the following parameters require specification:

(a) The size of monomers and oligomers;
(b) The generation rate of monomers and oligomers;

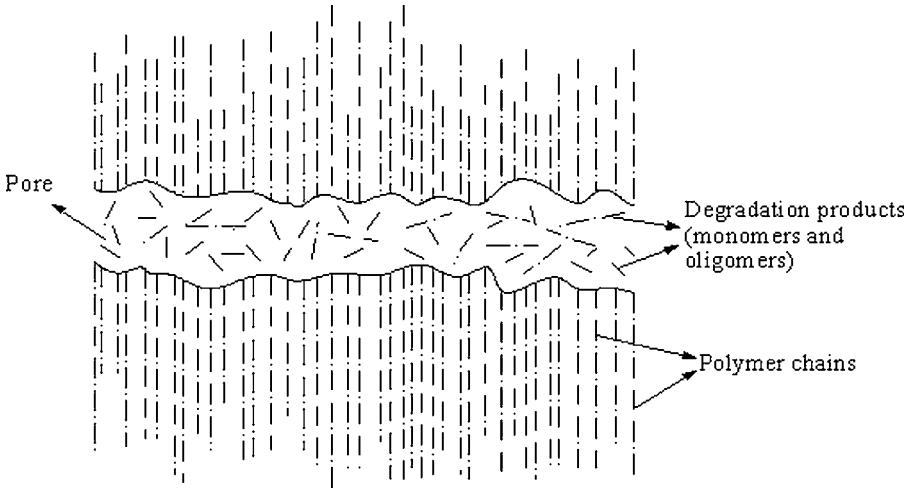

Figure 1. Illustration of the process of polymer erosion and pore growth.

(c) The diffusion rate of monomers and oligomers;
(d) The initial pore distribution.

The monomer and oligomer sizes can be estimated by the analysis of molecular structure, and the diffusion rate of monomers and oligomers through pore structures can be calculated by various transport models.[1–3,28] Therefore the polymer degradation rate remains the critical factor in predicting the transient pore size. However, as is well known, polymer degradation includes numerous spatially dependent chemical reactions that follow a random process.[10,29–31] In Batycky's theoretical work, polymer erosion was modeled as a process governed by both random chain scission and end scission.[23] To minimize complexity and still obtain reasonable predictability, we analyzed the transient pore evolvement using probabilistic methods.

Considering the polymer degradation mechanism, once a bond is broken in a linear polymer chain, end scissions, together with random chain scissions, become important in future degradation. Therefore, it is reasonable to assume that the generation of new pores is induced by random chain scissions, while the growth of an existing pore is attributed to both end chain scissions and random chain scissions. As we only consider the generation and growth of a single new pore, the pore coalescence will be neglected. The transient probability for end scissions (X_e) and the probability for internal chain scissions (X_i) are defined as polymer degradation variables over degradation time t. In the case of end scissions, only a specific u-mer is generated in unit time for cleavage. Here u represents the number of repeat units in a soluble oligomer or a monomer, which is also equal to the number of bonds to be cleaved from the polymer chain. However, for internal chain scissions, accounting for the growth of a certain pore, this cleavage must occur close to the pore, and, subsequently, at least two small molecules are generated in a given unit cleavage time. These small molecules are very likely to be different in size. In fact, the internal random chain scissions positioned far from a pore also affect the pore evolvement when the moving front of the pore gets closer to those points previously cleaved. It is also well known that the rate of end scission development is much faster than the rate of random chain scission development due to autocatalytic action. Consequently, end scissions dominate the degradation process close to an existed pore over a short time. With the ongoing degradation process, the influence of accumulated internal cleavages becomes more and more important for the pore evolvement. Thus, combining end scission and internal chain scission, the transient probability or rate of generating a specific u-mer attributed to the pore growth at time point t can be expressed as $f(u)$:

$$f(u) = X_e(1-X_e)^{u-1} + X_eX_i(1-X_i)^{u-1}\sum_{i=1}^{u_{max}}(1-X_e)^{i-1} + \cdots \quad (3)$$

where u_{max} is the maximum number of repeat units in a soluble oligomer cleaved from the polymer chain. In Eq. (3), the term $X_e(1-X_e)^{u-1}$ represents the transient probability of end scissions only; the term $X_eX_i(1-X_i)^{u-1}\sum_{i=1}^{u_{max}}(1-X_e)^{i-1}$ is a summation of all the cases that include one end scission plus an internal scission. Other internal scissions indirectly contributing to the pore growth are denoted by the suspension points.

As we know, pore growth is governed by numerous bond cleavages simultaneously along the axial direction of the pore; consequently the moving front of the pore would be irregular at different positions due to

the size variation of dissolved small molecules over time. Thus, the growing pore is expected to be asymmetric and there is a pore size distribution at various axial positions.[14] In order to characterize the average pore size, the parameter $\dot{u}_{ave}$ is defined as the average number of bonds for all the dissolvable monomers and oligomers generated per unit time. Then,

$$\dot{u}_{ave} = \sum_{u=1}^{u_{max}} uf(u) \tag{4}$$

Now we consider the size distribution of the polymer degradation products. We begin by defining the composition ratio of monomer A to monomer B in the copolymer as λ. The size of monomer A is denoted as l_A and the size of monomer B as l_B. The size of a monomer can be estimated by the composite bond lengths. Then the representative average length of the monomers, l_{ave}, is defined as:

$$l_{ave} = \frac{\lambda}{\lambda+1} l_A + \frac{1}{\lambda+1} l_B \tag{5}$$

giving the linear length of the soluble u-mer as ul_{ave}.

For constant l_{ave}, the pore size change can be described as

$$\frac{dR_p(t)}{dt} = l_{ave}\dot{u}_{ave} \tag{6}$$

where $R_p(t)$ represents the transient radius of a growing pore.

Therefore, we obtain

$$\frac{dR_p(t)}{dt} = l_{ave} \sum_{u=1}^{u_{max}} uf(u) \quad (t > 0) \tag{7}$$

Upon integration,

$$R_p(t) = l_{ave} \int_0^t \sum_{u=1}^{u_{max}} uf(u)\, dt + R_p(0) \tag{8}$$

For simplification we can define $D_f(t)$ as the combined distribution term that captures the effects of bond cleavages and degradation products:

$$D_f(t) = \int_0^t \sum_{u=1}^{u_{max}} uf(u)\, dt \tag{9}$$

Then the transient pore radius can be expressed as a function of this distribution term,

$$R_p(t) = D_f(t) l_{ave} + R_p(0) \tag{10}$$

Therefore, the transient pore radius can be simulated by the above model. Moreover, the significance of this work is the coupling of erosion kinetics to the pore radius as a function of time to subsequently predict the release rate, and the induction period for the microparticle payload release.

Assumptions Leading to Coupling Rate of $(u+1)$-mer Generation to Degradation Kinetics

The model outlined above can be used to predict general pore evolvement provided additional information, such as the specific rate of generation of $(u+1)$-mers, is provided or determined experimentally. In this work, we couple the rate of generating of oligomers and monomers to specific degradation kinetics. We do this by first relating the probability parameter $f(u)$ to polymer erosion kinetics. Here, we circumvent the kinetics complexity by invoking a number of appropriate assumptions.

Previous researchers have shown that, for a linear copolymer (-A-B-A-B-A-) or [-$(A)_i$-$(B)_j$-] such as PLGA-based copolymers, the apparent degradation kinetics follows the first-order expression:

$$-\frac{dM_n}{dt} = k_d t \tag{11}$$

where M_n is the number-average molecular weight of the polymer at degradation time, t, and k_d is the degradation constant determined directly from experiments.[30,32] The transient profile of M_n over time can be obtained from Eq. (11). The number of chain cleavages per initial number average molecule, denoted by x, is:

$$\frac{M_n^t}{M_n^0} = \frac{1}{1+x} \tag{12}$$

Here, M_n^t and M_n^0 refer to the number-average molecular weight of the polymer at time t and zero, respectively.[29,33] The apparent probability of the random bond cleavage, which may be viewed as the accumulated probability (X_t) of bond cleavages can be calculated by relating the accumulated probability to the initial number-average degree of polymerization (N). Then,

$$X_t = \frac{x}{N} \tag{13}$$

Now for every differential time element, it is assumed that the transient probability for bond cleavages contributes to the accumulated probability without probability transfer. Under this assumption, X_t is related directly to the independent transient probability $X(t)$ by

$$X_t = \int_0^t X(t)\, dt \tag{14}$$

Note that the independent transient probability of the random bond cleavage $X(t)$ is a function of time t. It is well known that the degradation rate varies with time due to a number of local factors such as transient proton concentrations and other transport phenomena. Consequently, the transient probability of bond cleavage, $X(t)$, is clearly time varying. In the general

model development, a transient probability of generating a u-mer at time point t is defined as $f(u)$. Since, $X(t)$ is a transient parameter which combines the total effects of degradation product distribution with bond cleavages, we assume that $X(t)$ can be used to approximate $f(u)$, or,

$$f(u) \approx X(t) \tag{15}$$

Here, assuming the equal probability of u-mer generation, we now relate the rate of generation of average number of bonds for all the dissolvable monomers and oligomers (Eq. 4), to obtain

$$\dot{u}_{\text{ave}} = \frac{u_{\max}+1}{2} X(t) \tag{16}$$

Approximating Pore Growing Rate to Degradation Kinetics

Substitute Eq. (16) into Eq. (6), we obtain

$$\frac{\mathrm{d}R_{\text{p}}(t)}{\mathrm{d}t} = \frac{(u_{\max}+1)l_{\text{ave}}}{2} X(t) \tag{17}$$

Therefore, we have

$$R_{\text{p}}(t) = \frac{(u_{\max}+1)l_{\text{ave}}}{2} \int_0^t X(t)\,\mathrm{d}t + R_{\text{p}}(0) \tag{18}$$

and,

$$R_{\text{p}}(t) = \frac{(u_{\max}+1)l_{\text{ave}}}{2N} \left(\frac{M_{\text{n}}^0}{M_{\text{n}}^t} - 1 \right) + R_{\text{p}}(0) \tag{19}$$

Thus the profile of $R_{\text{p}}(t)$ can be obtained theoretically when the above assumptions are valid. In Eq. (19), only M_{n}^t is a time dependent variable so we would expect an exponential growth behavior of the pore radius.

Relationship of Proposed Pore Growing Model to Previous Efforts

It is instructional to note that this model above correlates to previously obtained models if one assumes the transient probability $X(t)$ is time independent. Denoted by X, then we have the familiar expression:[23,24]

$$R_{\text{p}}(t) = \frac{(u_{\max}+1)l_{\text{ave}}}{2} X_t + R_{\text{p}}(0). \tag{20}$$

Use Hindered Transport to Model Protein Release from Degrading Microparticles

The above model emphasizes the pore size evolvement and applies to any general drug delivery carrier. To capture the rapid transition for protein delivery after an induction phase, we elect to use hindered transport theory to calculate an effective diffusion coefficient. With the transient pore radius $R_{\text{p}}(t)$, the hindered diffusion coefficient $D(t)$ is then calculated and related to diffusive protein release. Other hindrance models could also be used in this development. In this model, the point for sudden rapid increase in diffusion would be synonymous with an induction time where pore opening became sufficiently large to freely release previously encapsulated macromolecules.

For this model we use polyester-based microparticles that can undergo bulk erosion as the transport vehicle. Generally, this is a spherical particle characterized with a heterogeneous distribution of protein and pore structures.[12]

Based on the morphological features of the microparticles, we have the following assumptions for this system:

(1) Cylindrical pores in different size and tortuosity distribute heterogeneously in a microsphere with some interconnection. Protein molecules only distribute in the pore structures.
(2) During bulk erosion the average pore size begins to increase. At some position, inner pores develop into a protein reservoir.
(3) Initially, very few pores interconnect to the microparticle surface.
(4) During subsequent erosion, pores connecting to the exterior of the particle develop and enlarge over time. This is represented by $R_{\text{p}}(t)$ and is a function of polyester hydrolysis.
(5) The resulting protein molecules transport through the pores to the media via diffusion.
(6) Protein concentration variation caused by denaturation is neglected.

With the above assumptions, we further assume radial diffusion only. Therefore Fick's second law of diffusion in spherical geometry can be used to describe this system:

$$\frac{\partial C}{\partial t} = D_{\text{eff}}(t) \left(\frac{\partial^2 C}{\partial r^2} + \frac{2}{r} \frac{\partial C}{\partial r} \right) \tag{21}$$

with BCs:

$$r = 0, \quad \frac{\partial C}{\partial r} = 0 \tag{22}$$

$$r = R, \quad C = 0 \tag{23}$$

and IC:

$$t = 0, \quad C = C_0 \tag{24}$$

where $D_{\text{eff}}(t)$ is the effective diffusion coefficient calculated through hindered transport theory, C is transient protein concentration, C_0 is the initial protein concentration, r is the radius, and R is the particle size. Thus in this model, the initial pore is "loaded" with protein but transport is constricted due to hindrance until erosion increases the effective

diffusion to a point of transport. The induction time is estimated as the time required to reach this point.

To include the effects of protein transport through the serpentine channel, the tortuosity factor, τ, is introduced. The tortuosity factor is defined as unity when the polymer matrix collapses and generally ranges between 1 and 10.[34,35] However, it has been shown that, for PLGA or PLA microparticles, the tortuosity factor can be higher than 100.[36] In any case, combining the effect of tortuosity factor, the effective transient diffusion coefficient $D_{\text{eff}}(t)$ can be corrected by the following expression:

$$D(t)_{\text{eff}} = \frac{D(t)}{\tau} \tag{25}$$

where $D(t)$ is the hindered diffusion coefficient. For hindered transport in a growing pore, we now assume $D(t)$ varies with time due only to $H(t)$ and

$$D(t) = H(t)D_{\infty} \tag{26}$$

where $H(t)$ is the well-known centerline approximation hindrance factor

$$H(t) = \frac{6\pi(1-\lambda)^2}{9/4\pi^2\sqrt{2}(1-\lambda)^{-5/2}\left[1+\sum_{n=1}^{2} a_n(1-\lambda)^n\right] + \sum_{n=0}^{4} a_{n+3}\lambda^n} \quad (0<\lambda<1) \tag{27}$$

$$\lambda = \frac{R_{\text{d}}}{R_{\text{p}}(t)} \tag{28}$$

and D_{∞} refers to the diffusivity at infinite dilution.[22] The limiting effect of evolving pore size on drug transport is described by the variable λ, which is defined as the ratio of drug size R_{d} to the pore size $R_{\text{p}}(t)$ in Eq. (28). Thus the most significant factor in effecting the application of a hindered diffusion model in this study is determining the transient pore radius $R_{\text{p}}(t)$. Here, $R_{\text{p}}(t)$ can be obtained from the probabilistic model established above.

EXPERIMENTS AND METHODS

Materials

Poly (lactide-*co*-glycolide) (PLGA) 50:50, 75:25, and 85:15 (Resomer RG503, 755 and 858, Boehinger Ingelheim, Ingelheim, Germany) were obtained. The average molecular weights were 34k, 68k, and 220k, respectively. Ovalbumin (OVA) (Grade V, MW = 44k), bovine serum albumin (BSA) (Fraction V, MW = 64k), bicinchoninic acid (BCA) protein assay, and poly (vinyl alcohol) (PVA) (MW 30,000–70,000) were purchased from Sigma (St. Louis, MO). Methylene chloride (MC) was obtained from Fisher Scientific (Pittsburgh, PA).

Preparation of PLGA Microparticles

The microencapsulation procedure was based on double-emulsion (w/o/w) method.[12] PLGA was used as the wall polymer, protein as the encapsulating agents, MC as the organic solvent, and PVA as the emulsion stabilizer. The general experimental details are described elsewhere.[12] The microparticles were first frozen in liquid nitrogen and then freeze-dried (Freeze Dryer 4.5, Labconco, MO) at -50°C and 10 μm Hg overnight.

Characterization of PLGA Microparticles

After microencapsulation, the surface properties and general particle sizes were examined by scanning electron microscopy (SEM) (Hitachi S-4000, Tokyo, Japan). The particle size distribution was further analyzed by the software of Image J (Rasband, NIH, US Government) based on the images from SEM investigations. Total protein loadings and surface protein loadings of the microparticles were examined by standard methods.[37] The experimental details are described elsewhere.[12]

In Vitro Polymer Degradation and Protein Release

The microparticles were mixed with PBS buffer (pH 7.4, containing 0.02% sodium azide as a bacteriostatic agent) and incubated in an orbital shaker (Model 4520, Thermo Forma, Marietta, OH) under 37°C and 250 rpm. The vessels were carefully sealed to prevent water evaporation over a long period. For sampling, a small amount of supernatant after centrifuge was taken out of the incubation mixture. The protein release in the medium was measured by BCA protein assay at various time points. The incubation medium was frequently replaced by fresh PBS buffer to ensure a dilute solution for proteins and polymer degradation products. In addition, parallel experiments were performed to determine the effects of protein denaturation by incubating blank PLGA 50:50, 75:25, and 85:15 microparticles together with BSA solutions in a series of concentrations under exactly the same conditions. Protein release profiles were obtained by normalizing the apparent release data by the protein degradation results. Induction periods were estimated for each protein-polymer combination from the cumulative release curves. Each experiment was performed in triplicate.

RESULTS AND DISCUSSION

Experimental Protein Release Profiles and the Estimated Induction Periods

SEM analysis showed that the microparticles were spherical and smooth. The size distribution was

uniform in the range of 1–10 μm. Average particle sizes and size distribution with standard deviations are listed in Table 1. High protein surface loadings (>50%) were found with regard to total protein loadings (Tab. 2).

The *in vitro* protein release profiles of OVA-loaded and BSA-loaded PLGA microparticles are shown in Figures 2 and 3, respectively. As in the mathematical model, the influence of protein denaturation is not considered; therefore the effects of protein denaturation were eliminated by normalizing the apparent release data with the protein denaturation results.

OVA release profiles for PLGA 50:50 and PLGA 85:15 demonstrate a burst release (24.4% and 38.8%) in 1 day; while for PLGA 75:25, a small burst release (5.9%) was observed within the first day (Fig. 2). After 1 day of incubation, the release rate was dramatically reduced indicating that the prior rate was due to the transport of surface proteins. Although the microparticles formulated with PLGA 50:50 and PLGA 75:25 continued to demonstrate a slight but still continuous positive rate of protein release, we could still estimate an induction period for each type of microparticles. Assuming the induction period was between the burst release and the next significant positive change in release rate (the significant increase of release curve slope) for cumulative protein release, the induction periods were estimated to be 45, 70, and 105 days, respectively for the release of OVA from PLGA 50:50, 75:25, and 85:15 formulations.

Table 1. Average Particle Sizes of PLGA Microparticles in Different Monomer Ratios

Wall Polymers	Encapsulated Materials	Average Particle Size (μm)
PLGA 50:50	DI water	3.47 ± 1.39
	OVA	3.77 ± 1.37
	BSA	4.16 ± 1.49
PLGA 75:25	DI water	3.93 ± 1.44
	OVA	5.08 ± 1.97
	BSA	3.16 ± 0.70
PLGA 85:15	DI water	2.48 ± 0.52
	OVA	4.33 ± 1.41
	BSA	4.78 ± 1.72

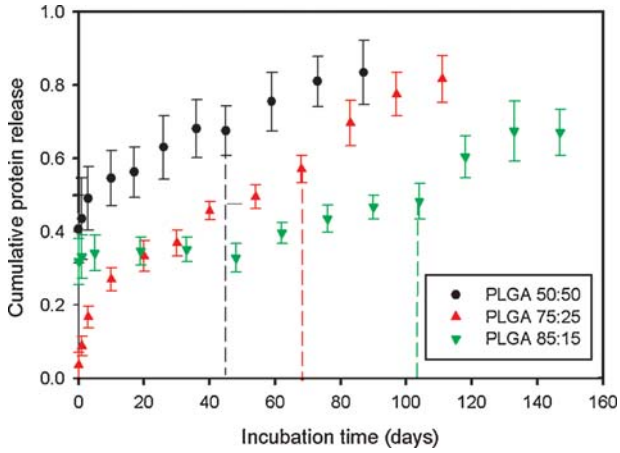

Figure 2. OVA release from PLGA microparticles in different monomer ratios (50:50, 75:25, and 85:15). The particles were fabricated using a double-emulsion method and incubated at 37°C at 250 rpm. Using the time between significant rate changes the induction periods for the PLGA 50:50, 75:25, and 85:15 microparticles are estimated to be 45, 70, and 105 days, respectively. The vertical colored lines are used to indicate the end of the induction period for each formulation.

The release profiles of BSA through the PLGA microparticles were slightly different than OVA release profiles (Fig. 3). A high burst release was observed within 1 day for all the three polymers (57.4%, 37.1%, and 43.7% for PLGA 50:50, 75:25, and 85:15, respectively). These values are higher than the corresponding cases using OVA but this is consistent with the higher BSA surface loadings relative to that of OVA surface loadings. Using the method to estimate the induction period described above in OVA release, the induction period for the release of BSA from PLGA 50:50, 75:25, and 85:15 microparticles were estimated to also be 45, 70, and 105, respectively. Protein release from different PLGA-formulated microparticles demonstrated a variation of release characteristics, such as the ratio of burst release, the occurrence and length of induction period, the occurrence and ratio of second pulse. These differences were caused not only by different monomer ratios in each wall polymer that

Table 2. Protein Loadings of the Microparticles for Various PLGA Formulations

	Protein Loaded/Particle Weights (w/w) (%), PLGA Ratio			Protein Loaded/Total Protein Used (%), PLGA Ratio			Surface Protein Loading (%) (mg protein/mg microparticles), PLGA Ratio			Surface Loading/Total Loading (%), PLGA Ratio		
Protein	50:50	75:25	85:15	50:50	75:25	85:15	50:50	75:25	85:15	50:50	75:25	85:15
OVA	5.6	5.2	5.0	65.4	60.6	58.7	3.28	3.15	3.29	58.5	60.7	65.4
BSA	4.8	5.0	5.3	55.8	57.8	61.5	3.34	3.95	4.41	69.7	79.6	83.5

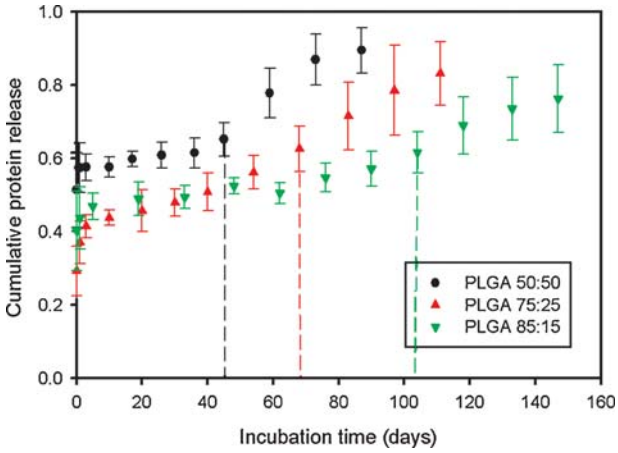

Figure 3. BSA release from PLGA microparticles in different monomer ratios (50:50, 75:25, and 85:15). The particles were fabricated using a double-emulsion method and incubated at 37°C at 250 rpm. Using the time between significant rate changes the induction periods for the PLGA 50:50, 75:25, and 85:15 microparticles are estimated to be 45, 70 and 105 days, respectively. The vertical colored lines are used to indicate the end of the induction period for each formulation.

led to different erosion kinetics, but also by the variation of initial and subsequent protein distribution profiles resulted from multiple microencapsulation processes.[14]

Theoretical Predictions of the Induction Periods

Here we apply our mathematical model to PLGA microparticles for prediction of the induction period. PLGA is a well-documented polyester undergoing bulk erosion. Lactic acid (LA) and glycolic acid (GA) are two monomer components for this copolymer. The sizes of LA and GA molecules are denoted by l_A and l_B, respectively. These values were estimated from the composite bond lengths and bond angles to give $l_A = 3.517$ Å, $l_B = 3.510$ Å. Using these values and Eq. (5), and the composition ratio of monomer A to monomer B, λ, (e.g., $\lambda = 3$ for PLGA 75:25), l_{ave} was calculated. Using the initial number-average molecular weight (M_n^0) of the polymer and the monomer molecular weight, the initial number-average of polymerization (N) was calculated. The degradation kinetics for all three PLGA ratios investigated was obtained from the literature. Table 3 summarizes the parameters used in the subsequent estimate of the pore evolution. The number of chain cleavages per initial number average molecule, x, was calculated and the accumulated probability, X_t, of bond cleavages over time t, $X_t \sim t$, was obtained from $t = 1$ day to $t = 90$, 120, 160 days depending on the time of complete degradation for each of the specific PLGA polymers. For PLGA polymers, the maximum number of bonds in a soluble oligomer (u_{max}) was documented as 9.[23] The tortuosity factor, τ, was assumed to be 3. Finally, the effective diffusion coefficient, $D(t)$ was determined using hindered transport theory.

Figure 4 shows the predicted effective diffusion coefficients for the PLGA microparticles for the release of simulated OVA and BSA. The induction period of protein release from PLGA microparticles obtained here is correlated to the point of rapid change in the effective diffusion coefficient. As a burst release was observed in the experiments due to surface protein release, in order to describe the induction period for the experimental results, we followed the convention and used the time duration between the initial burst and the most significant rapid change in release during the overall period. For the model prediction, the induction period was elected to be the time required for rapid change in the effective diffusion coefficient. From the theoretical calculations, the induction periods for OVA-loaded microparticles were estimated to be 45, 70, and 105 days for PLGA 50:50, 75:25, and 85:15 formulations, respectively; BSA-loaded microparticles had detectable induction periods as 50, 75, and 110 days for PLGA 50:50, 75:25, and 85:15 formulations, respectively. As can be seen, the induction periods estimated from theoretical simulations (summarized in Tab. 4) are in very good agreement with the values estimated from experiments.

The consistency of the theoretical simulations with experimental results demonstrates that the transient pore evolvement combined with hindered diffusion model works well to predict hindered protein release from PLGA microparticles undergoing bulk erosion. Given the simplicity of the model with respect to the complex erosion process and the particle size dis-

Table 3. Critical Parameters in Induction Period Prediction Model for PLGA Microparticles

Polymer	M_n	Initial Number of Bonds Per Polymer Molecule N	Average Monomer Size, l_{ave} (Å)	Degradation Rate Constant, k_d (day^{-1})
PLGA 50:50	20,462	314	3.514	−0.0773[a]
PLGA 75:25	40,366	588	3.515	−0.0622[a,b,c]
PLGA 85:15	108,647	1553	3.517	−0.0522[a,b,c]

The average monomer sizes were estimated from bond lengths and bond angles.
The available degradation rate constants for PLGAs varied between 0.02 and 0.1 day^{-1}. The values used in this calculation were obtained from: [a]Ref. 9, [b]Ref. 15 and [c]Ref. 30.

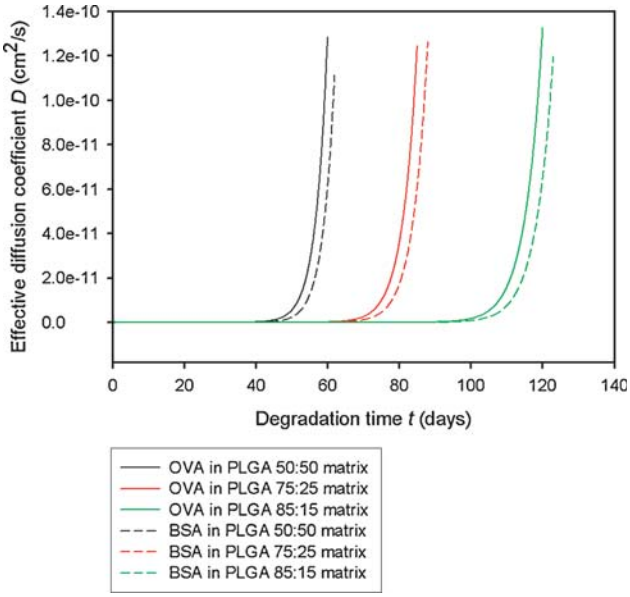

Figure 4. Model results for the transient effective diffusion coefficients of protein molecules in the growing pores of PLGA matrices calculated by hindered model. For OVA, $D_\infty = 7.2 \times 10^{-7}$ cm^2/s; for BSA, $D_\infty = 5.9 \times 10^{-7}$ cm^2/s. The point of onset for rapid change in the effective diffusion coefficient is used to indicate the end of the induction period for the modeled system.

tributions, these results correlate surprisingly well, albeit, the error may still on the order of days. This implies that the polymer degradation kinetics is the dominant contribution and can be correlated to the release rate for PLGA microparticles. It is reasonable that this theoretical simulation method can be extended to other polyester-based microparticles as well. In the time scale of an induction period, the effects of other phenomena, such as spontaneous pore coalescence and pore closing on pore evolvement are not significant, thus were ignored from this mathematical model. Pore coalescence can accelerate pore growth, while pore closing decelerate the apparent pore growth rate. The interactions of these two factors cause dissipation of both effects.

Table 4. Comparison of Estimated Induction Periods from Experiment (Figs. 2 and 3) and Model (Fig. 4)

Wall Polymer	Encapsulated Protein	Estimated Induction Period (Days)	
		Experimentally	Theoretically
PLGA 50:50	OVA	45	45
	BSA	45	50
PLGA 75:25	OVA	70	70
	BSA	70	75
PLGA 85:15	OVA	105	105
	BSA	105	110

As a matter of fact, pore coalescence rate/closing rates largely depend on the initial pore distribution profile and the followed pore growth rate. For the initial stage of bulk erosion, pore coalescence is not significant because the existed pores are insufficient for a large number of coalescence. In addition, polymer degradation and the subsequent pore growth dominate the induction period in bulk erosion; thus pore closing is negligible in this case. When degradation proceeds after the induction period, pore coalescence will become a significant factor which leads to fast drug release and particle matrix collapse. As our work is focused on pore evolvement in the induction period, this phenomenon is beyond our discussion.

Particle size (R) is also an important control parameter for drug release patterns not only through changes in diffusion rates but also through secondary effects including drug distribution in the particle, polymer degradation rate, and erosion rate of the particles.[36] Generally speaking, the reduced particle size will result in an increase of the surface area to volume ratio, which will speed up the buffer penetration into the particles and the escape of polymer degradation products. However, a more complex relationship was acknowledged between the particle size and protein release. First, a liner relationship between the polymer degradation rate and particle size was observed, with the larger particles degrading faster.[37] Later research shows that the degradation behavior of polymer matrix may not be significantly affected by the device size and the absolute release rate of the drug may increase with the increasing particle radius because large microparticles can become more porous during drug release than small microparticles, leading to higher apparent diffusivities and drug transport rates.[38] In our work, the effect of particle size (R) on induction time was investigated by this dynamic hindered diffusion model coupled with pore evolvement by variation of boundary condition in Eq. (23). A more complete evaluation requires a systematic study that combines both experimental evidence and a broad theoretical analysis.

In drug delivery system designs, the induction period is a crucial parameter that determines when the actual release starts. Especially for pulsatile release, such as the desirable single-shot vaccine for Hepatitis B, the induction period tells the length of waiting time between two pulses, which is vital with regard to the timeliness and effectiveness of boosting shot (releases). The mathematical modeling of induction period will provide meaningful information not only in selection of polymers, but also in designing the geometric structure of the particles to achieve the desirable drug release profile. Using this model, we can modulate important parameters for certain polyester-based protein delivery formulations

to optimize the drug release. More importantly, this model allows the prediction of the microparticle drug delivery induction time without direct experimental observations of the microparticle erosion.

CONCLUSIONS

A theoretical model for transient pore evolvement in biodegradable copolymer matrix based on polymer degradation kinetics and probability theory was developed. The transient pore evolvement, as captured by the effective diffusion coefficient of the protein in the copolymer matrix, is related to the distribution function of bond cleavages and degradation products. The effective diffusion coefficient in PLGA microparticles was modeled using hindered transport theory. The results showed that the theoretical estimates of the induction period were in very good agreement with experimental release studies of OVA and BSA from PLGA-formulated microparticles. The model is unique in that it can provide predictions of microparticle induction times without direct experimental microparticle erosion data. For systems in which the induction time may be on the order of months, this could provide a considerable benefit. In particular, this modeling approach can provide a substantial benefit for estimating booster times for single-shot vaccine devices.

REFERENCES

1. Siepmann J, Faisant N, Benoit JP. 2002. A new mathematical model quantifying drug release from bioerodible microparticles using Monte Carlo simulations. Pharm Res 19:1885–1893.
2. Siepmann J, Gopferich A. 2001. Mathematical modeling of bioerodible, polymeric drug delivery systems. Adv Drug Deliv Rev 48:229–247.
3. Faisant N, Siepmann J, Benoit JP. 2002. PLGA-based microparticles: Elucidation of mechanisms and a new, simple mathematical model quantifying drug release. Eur J Pharm Sci 15:355–366.
4. Knoll D, Hermans J. 1983. Polymer-protein interactions—Comparison of experiment and excluded volume theory. J Biol Chem 258:5710–5715.
5. Crotts G, Sah H, Park TG. 1997. Adsorption determines in-vitro protein release rate from biodegradable microspheres: Quantitative analysis of surface area during degradation. J Control Release 47:101–111.
6. Svergun DI, Richard S, Koch MHJ, Sayers Z, Kuprin S, Zaccai G. 1998. Protein hydration in solution: Experimental observation by x-ray and neutron scattering. Proc Natl Acad Sci USA 95:2267–2272.
7. Shanmugam G, Polavarapu PL. 2004. Vibrational circular dichroism spectra of protein films: Thermal denaturation of bovine serum albumin. Biophys Chem 111:73–77.
8. Colombo P, Bettini R, Santi P, DeAscentiis A, Peppas NA. 1996. Analysis of the swelling and release mechanisms from drug delivery systems with emphasis on drug solubility and water transport. J Control Release 39:231–237.
9. Pratt LR. 2002. Molecular theory of hydrophobic effects: "She is too mean to have her name repeated.". Annu Rev Phys Chem 53:409–436.
10. Chiu LK, Chiu WJ, Cheng YL. 1995. Effects of polymer degradation on drug release a mechanistic study of morphology and transport properties in 50:50 poly(dl-lactide-co-glycolide). Int J Pharm 126:169–178.
11. Sandor M, Enscore D, Weston P, Mathiowitz E. 2001. Effect of protein molecular weight on release from micron-sized PLGA microspheres. J Control Release 76:297–311.
12. Zhao AY, Rodgers VGJ. 2006. Using TEM to couple transient protein distribution and release for PLGA microparticles for potential use as vaccine delivery vehicles. J Control Release 113:15–22.
13. Kang JC, Schwendeman SP. 2007. Pore closing and opening in biodegradable polymers and their effect on the controlled release of proteins. Mol Pharm 4:104–118.
14. Hausberger AG, Deluca PP. 1995. Characterization of biodegradable poly(D,L-lactide-co-glycolide) polymers and microspheres. J Pharm Biomed Anal 13:747–760.
15. Shih C, Waldron N, Zentner GM. 1996. Quantitative analysis of ester linkages in poly(DL-lactide) and poly(DL-lactide-co-glycolide). J Control Release 38:69–73.
16. Reich G. 1997. Use of DSC to study the degradation behavior of PLA and PLGA microparticles. Drug Dev Ind Pharm 23:1177–1189.
17. Giunchedi P, Conti B, Scalia S, Conte U. 1998. In vitro degradation study of polyester microspheres by a new HPLC method for monomer release determination. J Control Release 56:53–62.
18. Reed AM, Gilding DK. 1981. Biodegradable polymers for use in surgery—Poly(ethylene oxide)-poly(ethylene terephthalate) (Peo-Pet) co-polymers. 2. In vitro degradation Polymer 22: 499–504.
19. Shih C. 1995. Calculation of hydrolytic rate constants of poly(-ortho ester)s from molecular weights determined by gel permeation chromatography. Pharm Res 12:2041–2048.
20. Arifin DY, Lee LY, Wang CH. 2006. Mathematical modeling and simulation of drug release from microspheres: Implications to drug delivery systems. Adv Drug Deliv Rev 58:1274–1325.
21. Beck RE, Schultz JS. 1972. Hindrance of Solute diffusion within membranes as measured with microporous membranes of known pore geometry. Biochim Biophys Acta 255:273–303.
22. Deen WM. 1987. Hindered transport of large molecules in liquid-filled pores. AIChE J 33:1409–1425.
23. Batycky RP, Hanes J, Langer R, Edwards DA. 1997. A theoretical model of erosion and macromolecular drug release from biodegrading microspheres. J Pharm Sci 86:1464–1477.
24. Lemaire V, Belair J, Hildgen P. 2003. Structural modeling of drug release from biodegradable porous matrices based on a combined diffusion/erosion process. Int J Pharm 258:95–107.
25. Barat A, Ruskin HJ, Crane M. 2008. 3D multi-agent models for protein release from PLGA spherical particles with complex inner morphologies. Theory Biosci 127:95–105.
26. Haas C, Drenth J, Wilson WW. 1999. Relation between the solubility of proteins in aqueous solutions and the second virial coefficient of the solution. J Phys Chem B 103:2808–2811.
27. Grassi M, Grassi G. 2005. Mathematical modelling and controlled drug delivery: Matrix systems. Curr Drug Deliv 2:97–116.
28. Saltzman WM, Pasternak SH, Langer R. 1987. Microstructural models for diffusive transport in porous polymers. ACS Symp Ser 348:16–33.
29. Kenley RA, Lee MO, Mahoney TR, Sanders LM. 1987. Poly(-lactide-co-glycolide) decomposition kinetics in vivo and in vitro. Macromolecules 20:2398–2403.
30. Sansdrap P, Moes AJ. 1997. In vitro evaluation of the hydrolytic degradation of dispersed and aggregated poly(DL-lactide-co-glycolide) microspheres. J Control Release 43:47–58.

31. Ramchandani M, Pankaskie M, Robinson D. 1997. The influence of manufacturing procedure on the degradation of poly-(lactide-co-glycolide) 85:15 and 50:50 implants. J Control Release 43:161–173.
32. Wu XS, Wang N. 2001. Synthesis, characterization, biodegradation, and drug delivery application of biodegradable lactic/glycolic acid polymers. Part II: Biodegradation. J Biomater Sci Polym Ed 12:21–34.
33. Inokuti M. 1963. Weight-average and Z-average degree of polymerization for polymers undergoing random scission. J Chem Phys 38:1174.
34. Higuchi T. 1963. Mechanism of sustained-action medication—Theoretical analysis of rate of release of solid drugs dispersed in solid matrices. J Pharm Sci 52:1145.
35. Zhang MP, Yang ZC, Chow LL, Wang CH. 2003. Simulation of drug release from biodegradable polymeric microspheres with bulk and surface erosions. J Pharm Sci 92:2040–2056.
36. Ehtezazi T, Washington C. 2000. Controlled release of macromolecules from PLA microspheres: Using porous structure topology. J Control Release 68:361–372.
37. Coombes AGA, Yeh MK, Lavelle EC, Davis SS. 1998. The control of protein release from poly(DL-lactide co-glycolide) microparticles by variation of the external aqueous phase surfactant in the water-in oil-in water method. J Control Release 52:311–320.
38. Siepmann J, Faisant N, Akiki J, Richard J, Benoit JP. 2004. Effect of the Size of Biodegradable Microparticles on Drug Release: Experiment and Theory. J. Controlled Release 96: 123–134.